

Molecular Catalysis of O Reduction by Iron Porphyrins in Water. Heterogeneous vs. Homogeneous Pathways.

Cyrille Costentin, Hachem Dridi, and Jean-Michel Savéant

J. Am. Chem. Soc., **Just Accepted Manuscript** • Publication Date (Web): 28 Sep 2015

Downloaded from <http://pubs.acs.org> on September 30, 2015

Just Accepted

“Just Accepted” manuscripts have been peer-reviewed and accepted for publication. They are posted online prior to technical editing, formatting for publication and author proofing. The American Chemical Society provides “Just Accepted” as a free service to the research community to expedite the dissemination of scientific material as soon as possible after acceptance. “Just Accepted” manuscripts appear in full in PDF format accompanied by an HTML abstract. “Just Accepted” manuscripts have been fully peer reviewed, but should not be considered the official version of record. They are accessible to all readers and citable by the Digital Object Identifier (DOI®). “Just Accepted” is an optional service offered to authors. Therefore, the “Just Accepted” Web site may not include all articles that will be published in the journal. After a manuscript is technically edited and formatted, it will be removed from the “Just Accepted” Web site and published as an ASAP article. Note that technical editing may introduce minor changes to the manuscript text and/or graphics which could affect content, and all legal disclaimers and ethical guidelines that apply to the journal pertain. ACS cannot be held responsible for errors or consequences arising from the use of information contained in these “Just Accepted” manuscripts.

Molecular Catalysis of O₂ Reduction by Iron Porphyrins in Water. Heterogeneous vs. Homogeneous Pathways.

Cyrille Costentin, Hachem Dridi and Jean-Michel Savéant**

cyrille.costentin@univ-paris-diderot.fr saveant@univ-paris-diderot.fr

Université Paris Diderot, Sorbonne Paris Cité, Laboratoire d'Electrochimie Moléculaire, Unité Mixte de Recherche Université - CNRS N° 7591, Bâtiment Lavoisier, 15 rue Jean de Baïf, 75205 Paris Cedex 13, France.

ABSTRACT. In spite of decades of active attention, important problems remain pending in the catalysis of dioxygen reduction by iron porphyrins in water in terms of selectivity and mechanisms. This is what happens e.g. for the distinction between heterogeneous and homogeneous catalysis for soluble porphyrins, for the estimation H₂O₂ / H₂O product selectivity and determination of the reaction mechanism in the two situations. Taking as example the water soluble iron tetrakis(N-methyl-4-pyridyl)porphyrin, procedures are described that allows one to operate this distinction and determine the H₂O₂/ H₂O product ratio in each case separately. It is noteworthy that, despite the weak adsorption of the iron (II) porphyrin on the glassy carbon electrode, the contribution of the adsorbed complex to catalysis rivals that of its solution counterpart. Depending on the electrode potential, two successive catalytic pathways have been identified and characterized in terms of current-potential responses and H₂O₂/ H₂O selectivity. These observations are interpreted in the framework of the commonly accepted mechanism for catalytic reduction of dioxygen by iron porphyrins, after checking its compatibility with a change of oxygen concentration and of *pH*. The difference in intrinsic catalytic reactivity between the catalyst in the adsorbed state and in solution is also discussed. The role of heterogeneous catalysis with iron tetrakis(N-methyl-4-pyridyl)porphyrin has been overlooked in previous studies because of its water solubility. The main thrust of the present contribution is therefore to call attention, by means of this emblematic example, on such possibilities so as to reach a correct identification of the catalyst, of its performances, and

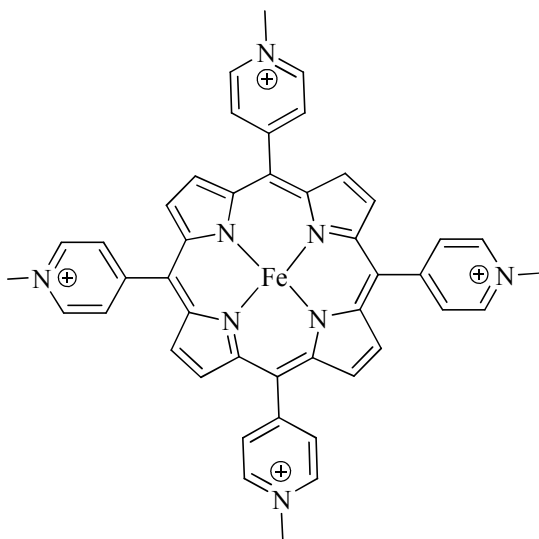
1 reaction mechanism. This is a question of general interest, the more so that reduction of dioxygen remains a
2 topic of high importance in the context of contemporary energy challenges.
3
4
5

6 Introduction

7
8
9 Molecular catalysis of the electrochemical reduction of dioxygen (ORR) has been the object of intense
10 research activity since a very long time and continues to attract active attention at present in resonance with the
11 biological importance of O₂ reduction and in electrochemical applications such as fuel cells.^{1,2,3} Metallo-
12 porphyrins have been extensively used in this purpose,⁴ notably iron porphyrins including in very recent
13 studies.^{5,6}
14
15
16
17
18
19

20
21 While many iron porphyrins used as ORR catalysts in non-aqueous organic solvents are soluble and
22 accordingly work as homogeneous catalysts, this is not the case in water where most studies concern molecules
23 absorbed onto the electrode surface, usually a carbon electrode, due to their low solubility. 4 The water-soluble
24 iron tetrakis(N-methyl-4-pyridyl)porphyrin (FeTMPyP, Chart 1) offers an interesting example where
25
26
27
28
29

30 Chart 1



31
32
33 an ORR homogeneous catalysis could be investigated in water.
34 However solubility in water does not a priori preclude some
35 adsorption and therefore the interference of heterogeneous
36 catalysis. It has been reported that the situation depends on the
37 nature of the particular carbon used as electrode material.^{7,8}
38
39
40
41
42
43
44
45
46
47
48
49
50

51 iron tetrakis(N-methyl-4-pyridyl)porphyrin (FeTMPyP)
52 not negligible, being of the same order of magnitude as the
53
54
55
56
57
58
59
60

homogeneous catalytic contribution to the current. This situation requires separation of the two contributions in
order to be able to estimate the H₂O₂/H₂O selectivity and to determine the kinetic characteristics of the two
catalytic pathways. As a preliminary, it was necessary to select the *pH* of the solution to avoid dimerization of

the FeTMPyP molecule. Cyclic voltammetry was used in the latter purpose as well as for mechanistic investigations. These were also carried out using rotating disk electrode voltammetry (RDEV) while rotating ring disk electrode voltammetry (RRDEV) was the main tool for estimating the H₂O₂/H₂O selectivity. One difficulty in the application of these techniques is the scarce solubility of dioxygen in water (1.4 mM at 20°C⁹), which restrains the conditions in which the current-potential response is not merely governed by oxygen diffusion.

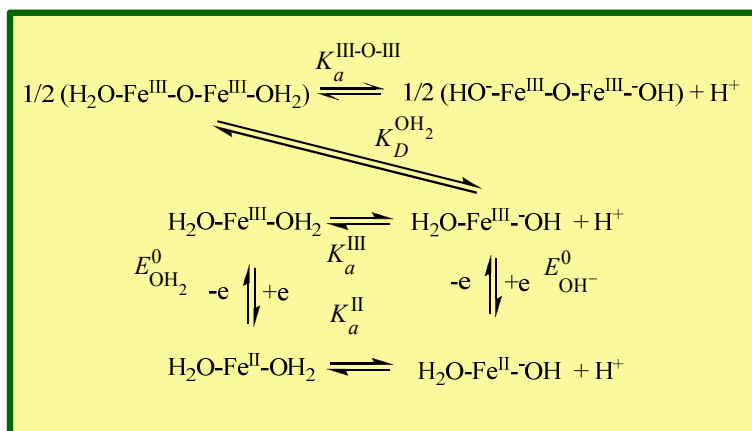
Instrumentation and procedures for application of these techniques are described in details in the Supporting Information (SI).

Results

1. Current-potential responses of the catalyst alone. How to avoid the interference of dimers?

Figure 1a shows the reversible cyclic voltammetry of Fe^{III}TMPyP in Britton-Robinson buffer (see SI) as a function of *pH*. A Pourbaix diagram (apparent standard potential vs. *pH*) can thus be derived from the variation of the middle potential between the cathodic and anodic peaks as represented in figure 1b. According to previous electrochemical and spectrochemical studies,^{7,10} the Pourbaix diagram responds to the equilibria shown in Scheme 1, which include the formation of μ -oxo dimers. The satisfactory fitting of the Pourbaix diagram (thick line in figure 1b) with the thermodynamic constants values listed in the caption of the figure confirms the validity of Scheme 1 as opposed to simple proton coupled electron transfer schemes (thin lines).

Scheme 1



It also allowed the calculations of the concentrations of the various monomeric and dimeric species present as a function of *pH* (see SI) leading to figure 1c.

We accordingly selected $pH = 3.8$ to carry out most of the following experiments because the solution then contains essentially the acid form of the iron(III) monomer (figure 1d) and that the reactions in which it could

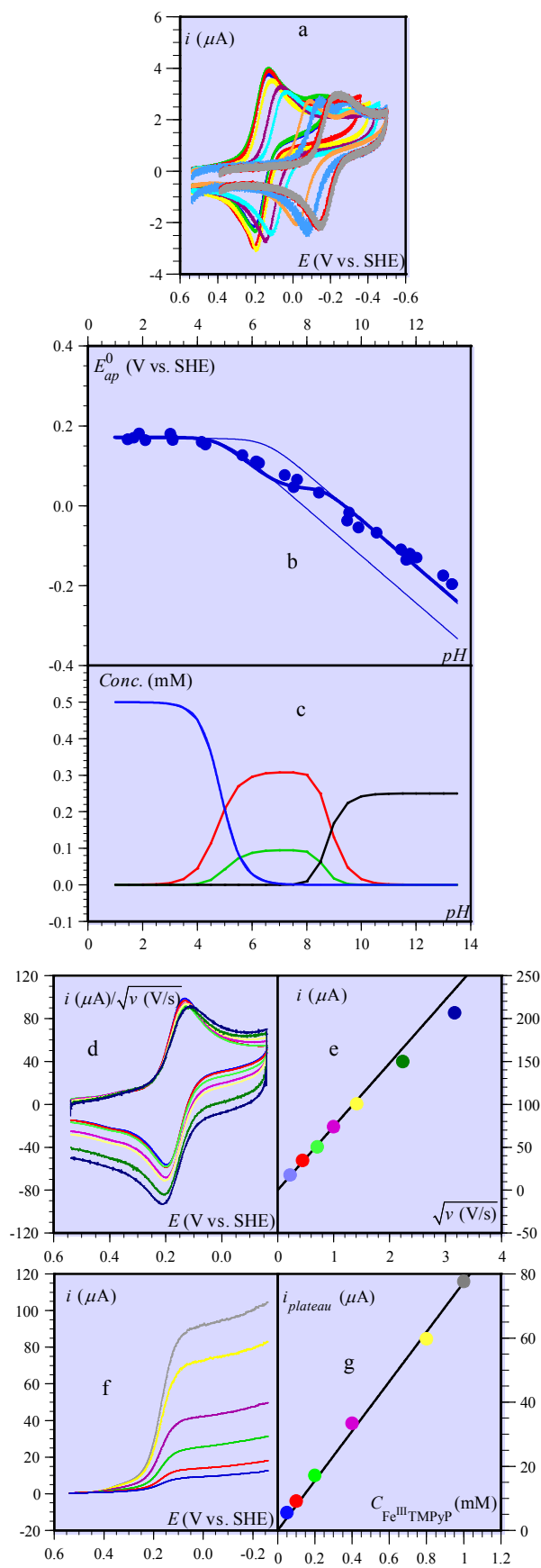


Fig. 1. a: cyclic voltammetry under argon of 0.5 mM Fe^{III}TMPyP in 0.04 M Britton-Robinson buffer as a function of *pH* on a 3 mm diameter GC electrode at 0.1 V/s (from left to right: *pH* = 1.7, 2.1, 3, 4.3, 6.1, 7.1, 10, 11.65, 13.0, 13.4). b: Pourbaix diagram obtained by plotting against *pH* the midpoints between cathodic and anodic peak potentials of the first wave of the cyclic voltammograms shown in figure 1a with additional data points deriving from cyclic voltammograms not shown in figure 1a for clarity. Thin lines: fitting for a simple ET-PT scheme with $E_{\text{OH}^-}^0 = 0.18$ V vs SHE; $pK_a^{\text{III}} = 5$ (left) and 6.5 (right). Thick line: fitting according to Scheme 1 for: $E_{\text{OH}^-}^0 = 0.18$ V vs SHE; $pK_a^{\text{III}} = 5$, $pK_a^{\text{II}} = 7$, $K_D^{\text{OH}_2} = 10^3$ (M^{-1/2}), $7^{10} pK_a^{\text{III-O-III}} = 8.5$. c: concentrations of H₂O-Fe^{III}-OH₂ (blue), H₂O-Fe^{III}-OH (red), H₂O-Fe^{III}-O-Fe^{III}-OH₂ (green), HO⁻-Fe^{III}-O-Fe^{III}-OH (black). d: cyclic voltammetry under argon of 1 mM Fe^{III}TMPyP in a 0.4 M acetate buffer +0.1 M KNO₃ at *pH* = 3.8 on a 5.6 mm diameter GC electrode; scan rate (V/s): 0.05 (blue), 0.2 (red), 0.5 (light green), 1 (magenta), 2 (yellow), 5 (dark green), 10 (dark blue). e: variation of the peak current in d with the scan rate. f: RDE voltammograms of Fe^{III}TMPyP at 2500 rpm in a 0.4 M acetate buffer +0.1 M KNO₃ at *pH* = 3.8 on a 5.6 mm diameter GC electrode as a function of concentration from top to bottom: 1, 0.8, 0.4, 0.2, 0.1, 0.05 mM. g: plateau current vs. concentration.

be involved are at equilibrium as shown by the proportionality of the cathodic peak to the square root of the scan rate (figures 1d and e). Likewise, the plateau currents of the RDE voltammograms show proportionality to the porphyrin concentration (figures 1f and g).

2. Current-potential responses of the catalyst alone. Is FeTMPyP adsorbed on glassy carbon (GC)?

As indicated previously, adsorption of FeTMPyP on GC is weak. We felt, however, useful to consider this point further, as it could be possible for the catalysis by the adsorbed catalyst to be nevertheless significant compared to its homogeneous counterpart if the Fe^{II} porphyrin is a more active catalyst in the adsorbed state in solution. As seen in figure 2a, a more careful examination of the FeTMPyP cyclic voltammetry reveals that a

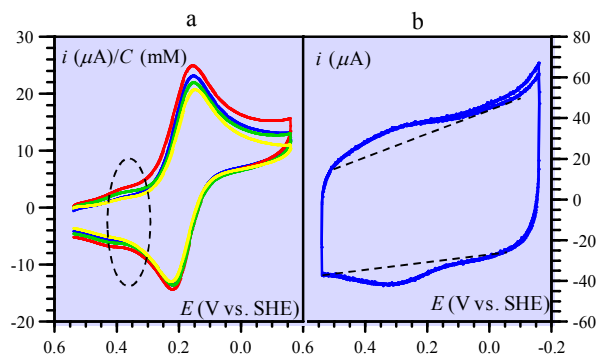


Fig. 2. a: cyclic voltammetry under argon of Fe^{III}TMPyP in a *pH* = 3.8-0.4 M acetate buffer + 0.1 M KNO₃ as a function of concentration (*C*) of Fe^{III}TMPyP at 0.05 V/s on a 5.6 mm GC electrode (*C* = 1, 0.8, 0.4, 0.2 mM). b: cyclic voltammetry of a GC electrode dipped in a 1 mM solution of Fe^{III}TMPyP in a *pH* = 3.8-0.1 M acetate buffer during 3 minutes, then pulled out, washed with the same buffer solution and transferred into a fresh buffer solution of the same composition with no-Fe^{III}TMPyP present. Scan rate: 5 V/s.

1 small pre-wave, which we have neglected so far, is present at the foot of the large diffusion wave. This prewave
2 may be assigned to an adsorbed $\text{Fe}^{\text{III}}/\text{Fe}^{\text{II}}$ couple, with the Fe^{II} form being more strongly adsorbed than the Fe^{III}
3 form.¹¹ This is confirmed by experiments in which the GC electrode is dipped in a $\text{pH} = 3.8$ 0.4 M acetate
4 buffer with $\text{Fe}^{\text{III}}\text{TMPyP}$ present during a few minutes, then pulled out, washed with the same buffer solution
5 and transferred into a fresh buffer solution of the same composition with no $\text{Fe}^{\text{III}}\text{TMPyP}$ present, showing a
6 small adsorption wave in the same potential range (figure 2b). This evidence of an adsorption of the
7 $\text{Fe}^{\text{III/II}}\text{TMPyP}$ couple will be taken into account in the discussion of the catalysis kinetics, based on a rough
8 estimate of the amount of catalyst adsorbed, $\Gamma^0 = 2 \times 10^{-11}$ M/cm² as sketched in figure 2b.
9
10
11
12
13
14
15
16
17
18

19 3. Reduction of O_2 alone on the same GC electrode and in the same buffer ($\text{pH} = 3.8$)

20
21 The investigation of O_2 alone on the same GC electrode in the same buffer was deemed necessary to estimate
22 the potential range where the catalytic reduction can be carried out with negligible interference of the direct
23 reduction at the electrode (figure 3a). It was also the occasion of determining the $\text{H}_2\text{O}_2 / \text{H}_2\text{O}$ product selectivity
24 of O_2 reduction at this pH by use of the RRDEV device (figures 3 b and c).
25
26
27
28
29
30

31 The apparent number of electrons exchanged, n_{ap} and the percentage of H_2O_2 formed can be derived from the
32 disk and ring current, i_{disk} and i_{ring} , according to the following equations (assuming no direct reduction of
33 H_2O_2 at the disk electrode).^{12a}
34
35
36
37
38
39
40
41
42
43
44
45
46
47
48
49
50
51
52
53
54
55
56
57
58
59
60

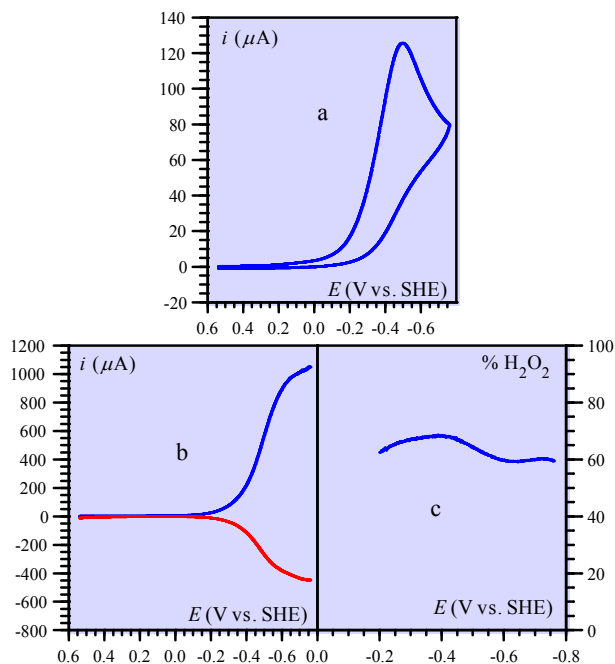


Fig. 3. a: cyclic voltammetry under 1 atm. O_2 in a $pH = 3.8-0.4$ M Britton-Robinson buffer at 0.05 V/s on a 5.6 mm GC electrode. b: RRDEV of the same solution at 2500 rpm and 0.05 V/s; blue curve: disk current as a function of potential; red curve: ring current/ N_{eff} as a function of the disk potential when the ring potential is poised at 1.04 V vs. SHE. c: percentage of H_2O_2 formed (see text).

$$\%H_2O_2 = 100 \frac{2i_{ring}}{i_{disk} + \frac{i_{ring}}{N_{eff}}}, \quad n_{ap} = \frac{4i_{disk}}{i_{disk} + \frac{i_{ring}}{N_{eff}}} \quad \text{and:} \quad \%H_2O_2 = 100 \frac{4 - n_{ap}}{2}$$

(N_{eff} is the collection efficiency¹²)

In the potential range where enough H_2O_2 is produced for a reasonably accurate determination to be possible,

$$\%H_2O_2 \approx 60 \quad \text{and} \quad n_{ap} = 2.8.$$

4. Catalysis of O_2 reduction by $Fe^{II}TMPyP$. General features.

Figure 4a shows the RDE catalytic voltammograms as a function of the rotation rate as compared to the voltammogram for the direct reduction of O_2 obtained at the highest rotation rate. There is a good separation in potential of the catalytic and direct reductions, thus allowing a detailed examination of the former process.

Figures 4a and 4b show that the current tends to vary proportionally to the square root of the rotation rate upon

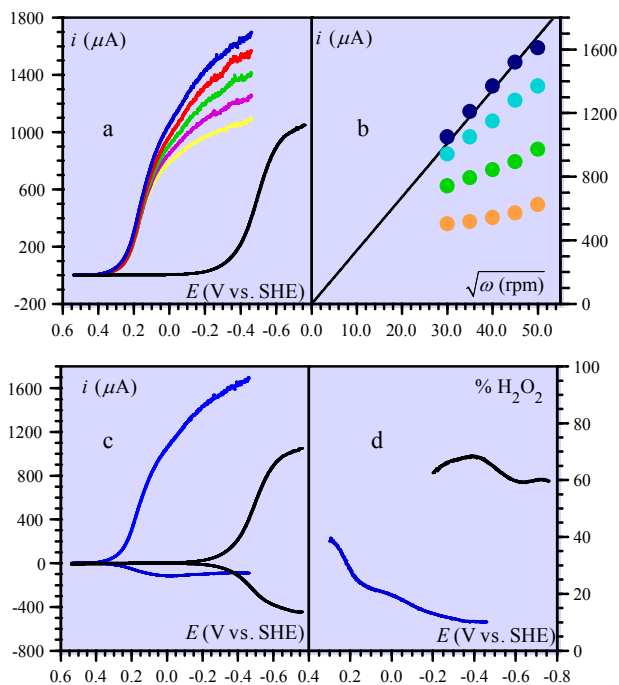


Fig. 4. a: RDEV of 1 mM Fe^{III} -TMPyP on a 5.6 mm GC electrode under 1 atm. O_2 in a $\text{pH} = 3.8$ - 0.4 M acetate buffer + 0.1 M KNO_3 as a function of the rotation rate (rpm): 900 (yellow), 1225 (magenta), 1600 (green), 2025 (red), 2500 (blue); 1 atm. O_2 alone in the same solution at 2500 rpm: black curve. $\nu = 0.05$ V/s b: variation of the current with the square root of the rotation rate as a function of the electrode potential (V vs. SHE): 0.14 (orange), 0.04 (green), -0.16 (cyan), -0.36 (dark blue). c: RRDEV of the same solution: upper blue curve: disk current as a function of potential; lower blue curve: ring current/ N_{eff} as a function of the disk potential when the ring potential is poised at 1.04 V vs. SHE for $\omega = 2500$ rpm. In black: the same curves for the direct reduction of O_2 (recall of figure 3b. d: apparent percentage of H_2O_2 formed.

going to negative potentials pointing to kinetic control by O_2 diffusion.¹³ Conversely, it is almost independent from the rotation rate at the foot of the catalytic wave indicating kinetic control by the catalytic reaction.¹³

We also note that the catalytic limiting current (blue curve in figure 4a) is larger than the O_2 direct reduction limiting current (black curve in figure 4a) at the same rotation rate (2500 rpm) indicating that the electron stoichiometry is larger in the first case than in the second. It follows that the $\text{H}_2\text{O}_2/\text{H}_2\text{O}$ product ratio in the catalyzed reduction is smaller than in the direct reduction. This is confirmed by the RRDEV experiments shown in figure 4c that shows that the catalytic ring current is smaller than the direct reduction ring current.

Another important feature of the catalytic responses is that they are actually composed of two successive waves as more clearly appears upon decreasing the catalyst concentration (figures 5a, b, c). The first wave is

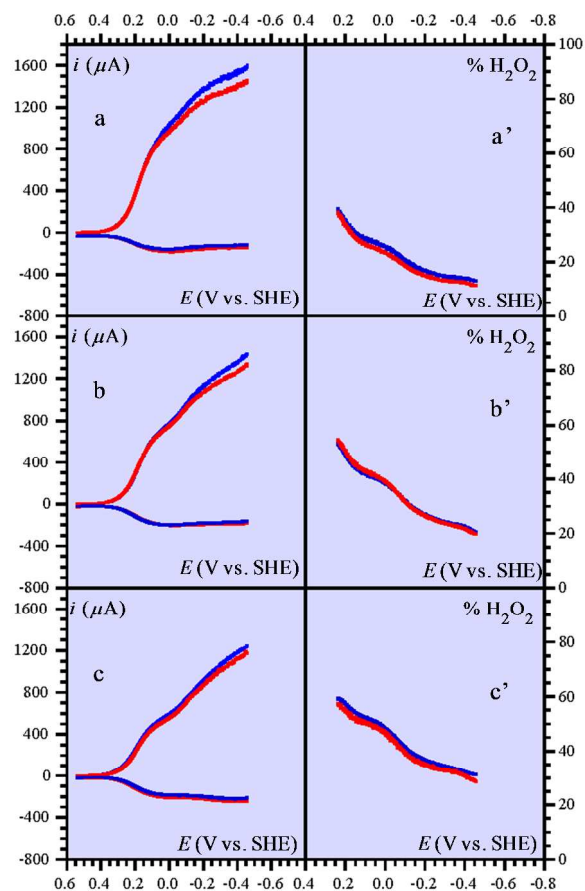


Fig. 5. a,b,c: RRDEV of $\text{Fe}^{\text{III}}\text{TMPyP}$ on a 5.6 mm GC electrode under 1 atm. O_2 in a $\text{pH} = 3.8$ -0.4 M acetate buffer as a function the catalyst concentration (mM) : a : 0.8, b: 0.4, c: 0.2, at 2500 (blue) and 2025 (red) rpm; upper curves: disk current as a function of potential; lower curves: ring current/ N_{eff} as a function of the disk potential when the ring potential is poised at 1.04 V vs. SHE. a',b',c': percentage of H_2O_2 formed under the same conditions.

under complete kinetic control by the catalytic reaction as follows from the independence of the current with respect to the rotational speed. It is also worth noting that the apparent $\text{H}_2\text{O}_2/\text{H}_2\text{O}$ product ratio is smaller at the second wave than at the first.

It is seen that at the foot of the catalytic wave the apparent $\text{H}_2\text{O}_2/\text{H}_2\text{O}$ product ratio rapidly drops. As shown later on, this is due to the fact that the foot of the catalytic wave is mainly due to heterogeneous catalysis which leads to higher $\text{H}_2\text{O}_2/\text{H}_2\text{O}$ product ratio than homogeneous catalysis.

A note of caution regarding the determination of product selectivity ratio $\text{H}_2\text{O}_2/\text{H}_2\text{O}$ from the RRDEV ring/disk current ratio is needed. Indeed during their travel from the disk, where they are generated, to the ring where they are detected, H_2O_2 molecules may undergo side-reactions that will minimize their production by the catalytic reaction taking place at the disk. One notable such side-reaction is the disproportionation of H_2O_2 triggered by

1 Fe^{III}TMPyP. The rate constant of this reaction is 10 M⁻¹s⁻¹ in acidic media,^{10a} meaning that for 1mM
2 Fe^{III}TMPyP, the pseudo-first order rate constant is 10⁻² s⁻¹. In a typical RRDEV set up as the one we have used
3 (see SI), the collection efficiency in presence of a coupled first order reaction, N_{eff}^k is given by:¹⁴
4
5
6

$$N_{eff} / N_{eff}^k = 1 + 1.28\nu / D_{H_2O_2}^{1/3} (k / \omega)$$

7
8
9
10
11 where ν is the viscosity of water (10⁻² cm²/s^{15a}), $D_{H_2O_2} = 1.7 \cdot 10^{-5}$ cm²/s the diffusion coefficient of H₂O₂.^{15b}
12
13 and k the first order rate constant. At a rotation rate of $\omega = 2500$ rpm, as mostly used in this work,
14
15
16
17 $N_{eff} / N_{eff}^k = 1.0024$, meaning that this reaction may be ignored in the following data treatment. This is not *a*
18
19 *priori* the case for the possible reduction of H₂O₂ by the Fe^{II}TMPyP complex generated at the disk electrode as
20
21 will be discussed in the following sections.
22
23

24 5. Catalysis of O₂ reduction by adsorbed FeTMPyP (heterogeneous catalysis).

25
26
27 We have seen, in section 2, that Fe^{III}TMPyP is weakly adsorbed on the GC electrode. Despite this modest
28
29 adsorption, does the corresponding heterogeneous catalysis contribute significantly to the overall catalytic
30
31 process is the question we address now. The answer is given by the experiments summarized in figure 6 and
32
33 described in the caption of this figure. It appears that the contribution of the heterogeneous process to the
34
35 overall catalysis is by no means negligible, the corresponding current being of the order of half the total
36
37 (compare figure 6 with figures 4 and 5). We also note that the H₂O₂/ H₂O product ratio is larger than in the
38
39 global catalysis process, being close to its value for the direct O₂ reduction.
40
41
42
43
44
45
46
47
48
49
50
51
52
53
54
55
56
57
58
59
60

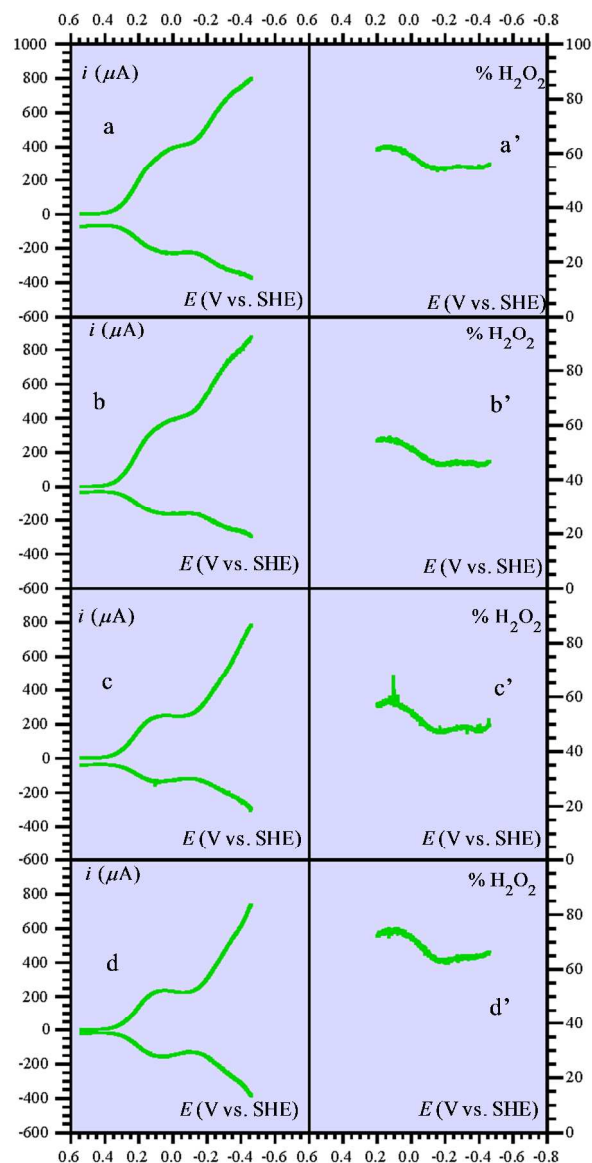


Fig. 6. a, b, c, d: RRDEV under 1 atm. O_2 of a 5.6 mm GC electrode dipped in solutions of $Fe^{III}TMPyP$ in a $pH = 3.8-4$ M acetate buffer during 15-20 minutes so as to reach the saturation adsorption corresponding to the solution concentration, then pulled out, washed with the same buffer solution and transferred into a fresh buffer solution of the same composition with no $Fe^{III}TMPyP$ present. $Fe^{III}TMPyP$ concentrations (mM): 1 (a), 0.8 (b), 0.4 (c), 0.2 (d). Rotation rate: 2500 rpm. $v = 0.05$ V/s. lower curves: ring current/ N_{eff} as a function of the disk potential when the ring potential is poised at 1.04 V vs. SHE. a', b', c', d': percentage of H_2O_2 formed under the same conditions.

Does all of the H_2O_2 produced at the disk electrode in the experiments of figure 6 reach the ring electrode or is part of it reduced by the $Fe^{II}TMPyP$ complex generated at the disk electrode? In other words, do the data displayed in the right part of figure 6 reliably represent the whole of the H_2O_2 molecules produced at the disk? The answer is provided by the experiments depicted in figure 7. $Fe^{II}TMPyP$ does catalyze the reduction of H_2O_2 produced at the disk electrode (figure 7a), but to a negligible extent as compared to the reduction of O_2 (figure

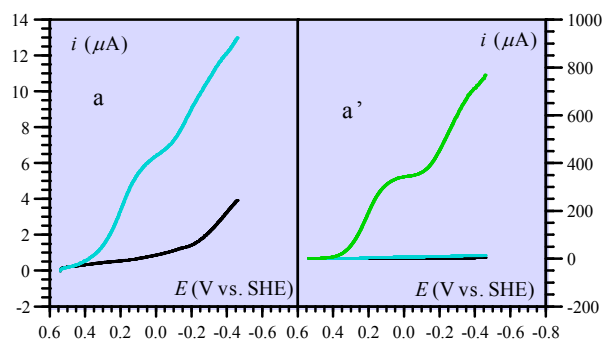


Fig. 7. RDEV of a 5.6 mm GC electrode dipped in solutions of $\text{Fe}^{\text{III}}\text{TMPyP}$ in a $pH = 3.8$ - 0.4 M acetate buffer during 10 minutes so as to reach the saturation adsorption corresponding to the solution concentration, then pulled out, washed with the same buffer solution and transferred into a fresh buffer solution of the same composition with no $\text{Fe}^{\text{III}}\text{TMPyP}$ present. Black curve: neither O_2 , nor H_2O_2 present; cyan curve: 1 mM H_2O_2 present in solution; green curve under 1 atm. O_2 .

7b).

We may therefore view the data in the right column of figure 6 as representing reliably the $\text{H}_2\text{O}_2/\text{H}_2\text{O}$ selectivity ratio of the heterogeneous catalytic reaction.

6. Homogeneous Catalysis of O_2 reduction by $\text{Fe}^{\text{II}}\text{TMPyP}$.

As seen in figure 5, the first catalytic wave is independent of the rotation rate, indicating that there is no interference of mass transport. It may thus be considered that, within the corresponding potential range, the heterogeneous and homogeneous contributions to catalysis are additive, the latter can be obtained by subtraction of the results of section 5 from those of section 4. The result is shown in figures 8a-d. As appears in figure 8e, at a given potential of the first wave (e.g. 0.04V vs. SHE), the homogeneous catalysis current varies, as expected, approximately proportionally to the catalyst concentration whereas the heterogeneous catalysis current remains constant as anticipated from the constancy of the saturation surface concentration of the catalyst. It should be noted that the subtraction procedure does not represent the exact contribution of homogeneous catalysis at potentials more negative than the first wave.

As discussed above, the reduction of H_2O_2 is not catalyzed appreciably by adsorbed $\text{Fe}^{\text{II}}\text{TMPyP}$. In experiments where $\text{Fe}^{\text{III}}\text{TMPyP}$ is present in the solution, the reduction of H_2O_2 produced both by heterogeneous and homogeneous catalysis of O_2 reduction, may however be catalyzed by the $\text{Fe}^{\text{II}}\text{TMPyP}$ molecules generated at the electrode, which diffuse away from the electrode. Detection at the ring will miss these H_2O_2 molecules and thus unduly minimize the $\text{H}_2\text{O}_2/\text{H}_2\text{O}$ product ratio. The following RDEV experiments (figure 8f) show that $\text{Fe}^{\text{II}}\text{TMPyP}$ does catalyze the reduction of H_2O_2 and that the reaction is endowed with a rate constant equal to ca. $10^4 \text{ M}^{-1} \text{ s}^{-1}$ (see SI). This reaction is fast, although slower than the reduction of O_2 by

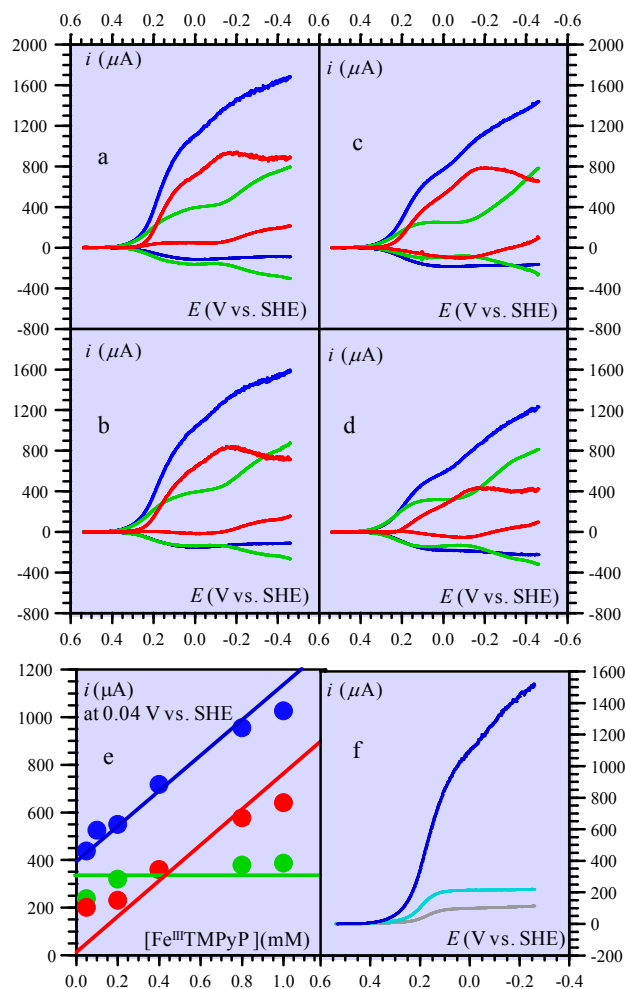


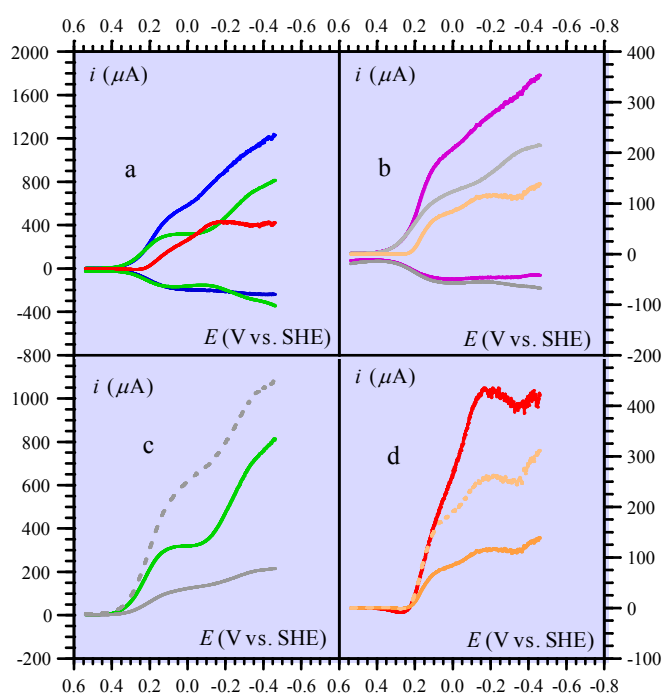
Fig. 8. a,b,c,d: construction of the homogeneous catalysis RRDEV responses under 1 atm. O₂ (red curves) by difference between the global catalysis responses (blue curves as in figure 4c and 5 a, b, c) and the heterogeneous catalysis RRDEV responses (green curves as in figure 6); Fe^{III}TMPyP concentrations (mM): 1 (a), 0.8 (b), 0.4 (c), 0.2 (d). Rotation rate: 2500 rpm. e: current at 0.04 V vs. SHE versus catalyst concentration for global catalysis (blue dots), heterogeneous catalysis (green dots) and homogeneous catalysis (red dots). (f): REDV at 2500 rpm of 1 mM Fe^{III}TMPyP in a pH = 3.8-0.4 M acetate buffer under argon (grey), in the presence of 1 mM H₂O₂ (cyan) and under 1 atm. O₂ (blue).

Fe^{II}TMPyP (figure 8f). Pure kinetics behavior observed at high rotation rate implies that reduction reactions are taking place within a reaction layer adjacent to the disk electrode. The thickness of this reaction layer is governed by the fastest reaction which is here O₂ reduction (this can be inferred from the relative current for O₂ and H₂O₂ reductions in RDEV in comparable concentrations). Outside this reaction layer, H₂O₂ only diffuses and may reach the ring electrode. Consequently, the ring current is relative to the amount of H₂O₂ escaping the reaction layer. The size of this reaction layer is much smaller than the distance between the disk electrode and the ring electrode. Therefore, the molecules H₂O₂ effectively collected at the ring, i_{ring} / N_{eff} is related to the flux that escape the reaction layer. Determination of the fraction of H₂O₂ that escapes reduction of H₂O₂ in the

1 reaction layer requires knowing the mechanism. This is the reason that analysis of $\text{H}_2\text{O}_2/\text{H}_2\text{O}$ selectivity for the
 2 homogenous catalysis is postponed after a mechanism is proposed, which requires examining first the effects of
 3 O_2 concentration and $p\text{H}$ on the catalytic current.
 4
 5
 6

7. Effect of O_2 concentration.

9 The effect of dioxygen concentration on the heterogeneous and homogeneous catalysis is examined by
 10 comparison of the RDEV and RRDEV curves obtained under 1 atm. O_2 (figure 9a) and air (figure 9b). The
 11 amount of H_2O_2 formed, as reflected by the ring current is almost entirely due to the heterogeneous processes in
 12 both cases (figure 9a and 9b). The corresponding selectivity is *ca.* 55% H_2O_2 under O_2 and 50% H_2O_2 under air.
 13
 14
 15
 16
 17
 18



19
 20
 21
 22
 23
 24
 25
 26
 27
 28
 29
 30
 31
 32
 33
 34
 35
 36
 37
 38
 39
 40
 41
 42 Fig. 9. RRDEV of a 0.2 mM solution $\text{Fe}^{\text{III}}\text{TMPyP}$ in a $p\text{H} = 3.8-0.4$ M acetate buffer (rotation rate: 2500 rpm).
 43 **a**: under 1 atm. O_2 ; blue curves: global catalysis, green curves: heterogeneous catalysis as in figure 6, red
 44 curves: homogeneous catalysis obtained by difference between the blue and green curves. **b**: in air; magenta
 45 curves: global catalysis; grey curves obtained as in **a** but in air instead of 1 atm. O_2 ; orange curves:
 46 homogeneous catalysis obtained by difference between the magenta and grey curves. **c**: heterogeneous catalysis
 47 under 1 atm. O_2 (green as in **a**) and air (grey as in **b**, dotted grey: $\times 5$). **d**: homogeneous catalysis under 1 atm.
 48 O_2 (red curve as in **a**) and air (orange as in **b**, dotted orange: $\times \sqrt{5}$)
 49
 50

51 The heterogeneous catalysis disk current is clearly dependent on the O_2 concentration (figure 9c). It varies
 52 less than proportionally to $[\text{O}_2]$. This observation indicates that the addition of O_2 on the Fe^{II} porphyrin,
 53 although it clearly interferes in the catalysis kinetics, is neither the rate-determining step nor a pre-equilibrium
 54
 55
 56
 57
 58
 59
 60 of the rate-determining step.

Assuming, as above, the additivity of the heterogeneous and homogeneous contributions, the latter is obtained by subtraction of the former from the global catalysis response, leading to the red and orange curves in figures 9a and 9b and in figure 9d. The first wave current is proportional to $\sqrt{[O_2]}$, indicating that the addition of O_2 on the Fe^{II} porphyrin is either the rate-determining step or a pre-equilibrium of the rate-determining step.¹⁶ This assertion also falls in line with the observation that the half-wave potential is equal to the standard potential of the Fe^{III}/Fe^{II} couple.^{16c} At potential more negative than -0.1 V O_2 mass transport starts to interfere significantly. The variation of the current with O_2 concentration is then more important than proportionality to $\sqrt{O_2}$ thus explaining why an apparent increase of the reaction order with respect to O_2 is observed.

8. Dependence toward pH.

The previous RRDEV experiments were repeated at a pH of 1.15 in order to gauge the effect of pH on the kinetics of catalysis and on the H_2O_2/H_2O selectivity ratio.¹⁷ It is seen (figure 10) that there is practically no effect of pH on the heterogeneous and homogeneous catalytic RDEV waves. The same is true for the RRDEV waves, indicating the H_2O_2/H_2O selectivity ratio does not vary appreciably in this pH range.

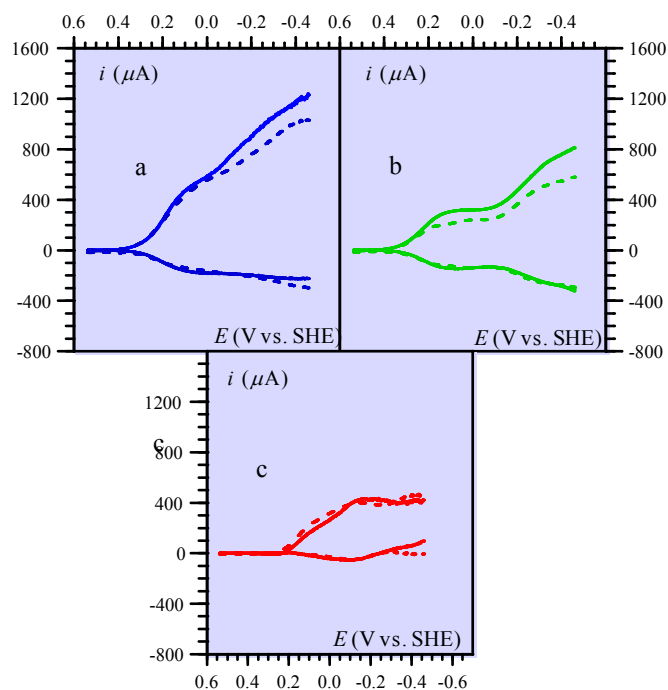


Fig. 10. RRDEV (rotation rate: 2500 rpm) of a 0.2 mM solution Fe^{III} -TMPyP at $pH = 3.8$ -0.4 M acetate buffer (full line) and $pH = 1.15$ (dashed line) under 1 atm. O_2 . **a**: global catalysis. **b**: heterogeneous catalysis. **c**: homogeneous catalysis

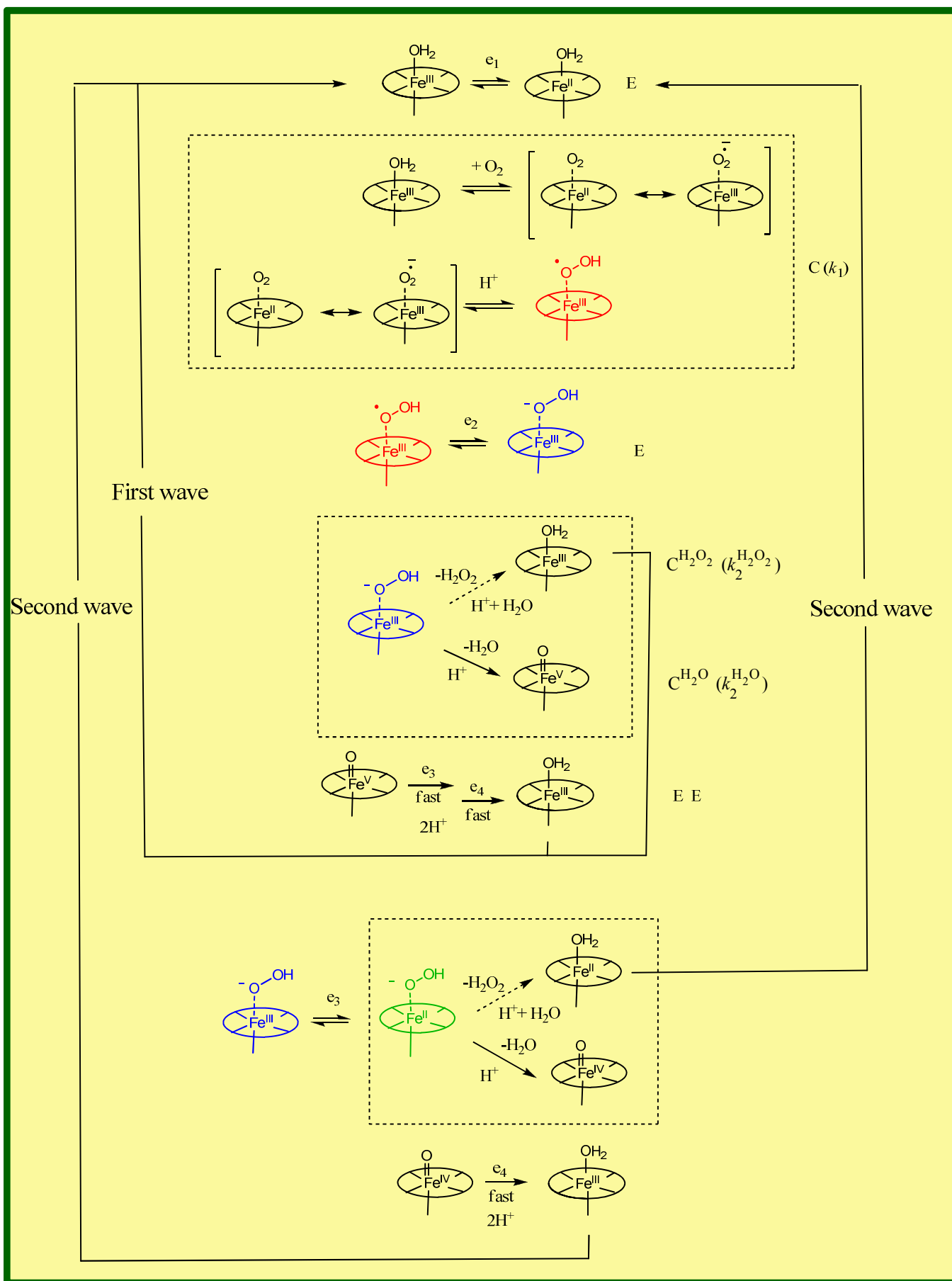
Discussion

The most striking of our observations, at variance with previous reports,^{8,10} is that the Fe^{III/II}TMPyP couple catalyzes O₂ reduction not only in solution but also at the adsorbed state when using glassy carbon as electrode material. In spite of the weak adsorption of both members of the couple, the contributions of heterogeneous and homogeneous catalysis are of similar magnitude. An analysis of the kinetics of the two catalytic regimes is required to know whether this observation is related either to an intrinsic difference of reactivity or to the involvement of different amounts of catalytic material in the two cases or to a combination of these two factors. Before addressing this point it is worth summarizing the characteristics of each of the two catalytic regimes so as to establish of reaction sequence they entail. We note in this regard that the second important finding of the present study is that both heterogeneous and homogeneous catalysis regimes give rise to two successive waves. In both cases, the first of these occurs around the standard potential of the Fe^{III/II}TMPyP couple. The second, more negative, wave is likely to involve the reduction of an intermediate formed at the first wave.

The main characteristics of the heterogeneous catalytic process are: (i) the O₂ reaction order at the first wave is less than 1; (ii) the *pH* has no noticeable effect on the first wave; (iii) selectivity: *ca* 60% H₂O₂, 40% H₂O, independent of *pH* and [O₂]. Using the intermediate species commonly invoked in the reduction of dioxygen by Fe^{II} porphyrins,⁴ these observations suggest the mechanism depicted in Scheme 2. After the initial electron transfer, which converts the starting Fe^{III} porphyrin into the Fe^{II} porphyrin, the complex resulting from the addition of O₂ on the latter is protonated giving rise to the intermediate noted in red in the Scheme. As in most ECE-type mechanisms driven by a protonation reaction, the resulting protonated species is easier to be reduced than the starting molecule.¹⁸ This second E-step produces the intermediate noted in blue, which is at the crossroad of product selection for the first wave catalysis and whose reduction triggers the second catalytic wave. In the framework of these ECEC (forming H₂O₂) or ECECEE (forming H₂O) reaction pathways, the plateau current of the first wave, *i*_{pl}, and its half-wave potential, may be expressed by (see SI) :

$$\frac{i_{pl}}{FS} = n_{ap} \frac{\Gamma^{-0}}{\frac{1}{k_1^{het}} + \frac{1}{k_{2,H_2O_2}^{het} + k_{2,H_2O}^{het}}} \quad (1)$$

Scheme 2



$$\text{with } n_{ap} = 4 - 2 \left(\frac{\%H_2O_2}{100} \right)$$

$$E_{1/2} = E_{cat}^0 + \frac{RT}{F} \ln \left(1 + \frac{k_1^{het}}{k_{2,H_2O_2}^{het} + k_{2,H_2O}^{het}} \right) \quad (2)$$

as function of the global rate constant, k_1^{het} , of the first two steps following the initial electron transfer and of the two rate constants, $k_{2,H_2O_2}^{het}$ and k_{2,H_2O}^{het} , of the H_2O_2 and H_2O forming steps, respectively (Γ^0 is the surface concentration of catalyst and E_{cat}^0 , the standard potential of the catalyst couple). i_{pl} depends on the O_2 concentration, but with a reaction order smaller than 1. The observation that the 1st wave current does not depend on pH , shows that the addition of O_2 on the Fe^{II} porphyrin is irreversible, presumably so because of rapid protonation of the addition complex. Bond cleavages in the second C-steps are likewise irreversible, possibly due to rapid follow-up protonation in this case too. The mechanism is completed by the reduction of the blue intermediate at a more negative potential, giving rise to the green intermediate, which splits in a similar manner although somewhat more in favor of H_2O_2 .

Because the plateau current is not proportional to $[O_2]$ and because the half-wave potential is not far from E_{cat}^0 , we may consider that $k_1^{het} \approx k_{2,H_2O_2}^{het} + k_{2,H_2O}^{het}$ and thus that:

$$\frac{i_{pl}}{FS} \approx \frac{n_{ap}}{2} k_1^{het} \Gamma^0 \quad (3)$$

Application of equation (3) to the data displayed in figure 8e (green dots) leads to $k_1^{het} \approx 780 \text{ s}^{-1}$.

Turning now to the homogeneous catalytic process, its main characteristics are: (i) the O_2 reaction order at the first wave is 1 and half-wave potential is equal to the standard potential of the Fe^{III}/Fe^{II} couple (ii) the pH has no noticeable effect on the first wave; (iii) a direct estimation of the selectivity ratio from ring / disk currents ratio is not possible because reduction of H_2O_2 has to be considered.

For the same reasons as for the heterogeneous case, the mechanism sketched in Scheme 2 is applicable here to with the difference that addition of O_2 to the Fe^{II} complex is irreversible and rate determining ,i.e., (

$k_1^{hom} \ll (k_{2,H_2O_2}^{hom} + k_{2,H_2O}^{hom})$. The second catalytic process is triggered by the reduction of the blue intermediate, which is easier to reduce than when it is adsorbed on the electrode, presumably because of a stronger axial ligation in the adsorbed state. As already mentioned, the reduction of H_2O_2 produced both by heterogeneous and homogeneous catalysis of O_2 reduction, is catalyzed by the $Fe^{II}TMPyP$ molecules generated at the electrode, which diffuse away from the electrode. Detection at the ring will miss these H_2O_2 molecules and thus unduly minimize the H_2O_2/H_2O product ratio. However, focusing on the first wave, it can be shown that the disk current is given by (see SI):

$$\frac{i}{FS} = \frac{i_{het}}{FS} + \frac{2 \left(1 + \frac{k_{2,H_2O}^{hom}}{k_{2,H_2O_2}^{hom} + k_{2,H_2O}^{hom}} \frac{k_1^{hom}}{k_1 + k_3 [H_2O_2]} \right) \sqrt{D_{cat} (k_1^{hom} + k_3 [H_2O_2])} C_{cat}^0}{1 + \frac{\sqrt{k_1^{hom} + k_3 [H_2O_2]}}{\sqrt{k_{2,H_2O_2}^{hom} + k_{2,H_2O}^{hom}}} \left(\frac{k_1^{hom}}{k_1^{hom} + k_3 [H_2O_2]} \right) + \exp \left[\frac{F}{RT} (E - E^0) \right]} \quad (4)$$

where k_3 is the rate constant for H_2O_2 reduction by $Fe^{II}TMPyP$ and $[H_2O_2]$ the concentration of H_2O_2 in the reaction layer at a given potential. Because it is observed experimentally that (i) the homogeneous contribution of the disk current is proportional to $\sqrt{[O_2]}$, i.e to $\sqrt{k_1^{hom}}$, and (ii) the half-wave potential is very close to E^0 , we conclude that in our experimental conditions: $k_1^{hom} \gg k_3 [H_2O_2]$ and $\sqrt{k_1^{hom}} \gg \sqrt{k_{2,H_2O_2}^{hom} + k_{2,H_2O}^{hom}}$. Then the plateau current for the homogeneous contribution to the disk current is:

$$\frac{i_{pl}^{hom}}{FS} = n_{ap} C_{cat}^0 \sqrt{D_{cat}} \sqrt{k_1^{hom}} \quad (5)$$

$$\text{with } n_{ap} = 4 - 2 \left(\frac{\%H_2O_2}{100} \right) \text{ and } \left(\frac{\%H_2O_2}{100} \right) = \frac{k_{2,H_2O_2}^{hom}}{k_{2,H_2O_2}^{hom} + k_{2,H_2O}^{hom}} = \frac{\frac{2i_{ring}^{hom}}{N_{eff}}}{i_{disk}^{hom} + \frac{i_{ring}^{hom}}{N_{eff}}}$$

The ring current for the homogeneous catalysis is finally obtained by subtracting to this corrected ring current the contribution from the heterogeneous catalysis (figure 8). It thus appears that this ring current is small and not easy to measure, indicating selectivity smaller than 20%. This estimation is very approximate and has no

1 other merit than to indicate that the $\text{H}_2\text{O}_2/\text{H}_2\text{O}$ -selectivity ratio for homogeneous catalysis is clearly less than
2
3 for heterogeneous catalysis.

4
5 Application of equation (5) to the data displayed in figure 8e (red dots) leads to $k_1^{hom} \approx 30 \text{ s}^{-1}$.¹⁹

6
7
8 It is interesting to note that equation may be rewritten as:

9
10
11
$$\frac{i_{pl}}{FS} = n_{ap} \left(C_{cat}^0 \sqrt{\frac{D_{cat}}{k_1^{hom}}} \right) k_1^{hom}$$

12
13
14
15 where $\sqrt{D_{cat}/k_1^{hom}}$ is the thickness of the catalytic reaction-diffusion layer (see SI) where the molecules that
16
17 actually partake to the catalytic process are located. $C_{cat}^0 \sqrt{D_{cat}/k_1^{hom}}$ is thus the surface concentration of the
18
19 molecules effectively partaking to the catalytic process, to be compared with Γ^0 in heterogeneous catalysis (
20
21 2×10^{-10} vs. $2 \times 10^{-11} \text{ M/cm}^2$).²⁰

22
23
24
25
26
27 These differences between the two catalytic regimes have been taken into account in the above estimation of
28
29 the rate constants, the ratio of 26 in favor of the heterogeneous pathway therefore does represent an actual and
30
31 significant difference in reactivity, even though several parameters have been estimated rather crudely. A
32
33 plausible interpretation of the increased efficiency of heterogeneous vs. homogeneous catalysis is that it may be
34
35 related to a better ligation of the complex at the adsorbed state, presumably by ligands present on the GC
36
37 surface, than by the ligands available in solution.²¹ This better ligation is expected to favor the rate formation of
38
39 the initial $\text{Fe}^{\text{II}}\text{O}_2$ ($\text{Fe}^{\text{III}}\text{O}_2^{\bullet-}$)²² and therefore catalytic efficiency. A better ligation by ligands present on the GC
40
41 surface, than by the ligands available in solution may also be inferred from the fact that the standard potential of
42
43 the adsorbed couple is *ca* 120 mV more positive than its homogenous counterpart.
44
45
46
47
48

49
50 This likely explanation of the differences and similarities between the heterogeneous and homogeneous
51
52 catalysis by FeTMPyP has assumed that the same iron porphyrin molecule as in solution is adsorbed on the
53
54 electrode surface, albeit with some difference in axial ligation. This assumption is based on the proximity of the
55
56 standard potentials and on the fact that the heterogeneous catalytic response has the same features as its
57
58 homogeneous counterpart, including the detection of H_2O_2 as a product. A spectroscopic characterization of the
59
60

1 adsorbed porphyrin seems out of reach at present in view of the smallness of the amount adsorbed. In this
2 connection, we may note that the spectroscopic characterization of the very same porphyrin adsorbed within a
3 mesoporous TiO₂ electrode (where adsorption is much more massive) has recently²³ revealed no major changes
4 in the porphyrin spectrum compared to the solution molecule.
5
6
7
8

9 **Conclusion**

10 The main finding of this revisitation of the catalysis of O₂ reduction by iron (II) tetrakis(N-methyl-4-
11 pyridyl)porphyrin, at variance with previous studies, is that, despite the weak adsorption of the iron (II)
12 porphyrin on the glassy carbon electrode, the contribution of the adsorbed complex to catalysis is of the same
13 order of magnitude as that of its solution counterpart.
14
15
16
17
18
19

20 In both regimes, the first steps of the reaction sequence involve the formation of an Fe^{II}-O₂ adduct that is
21 rapidly protonated and reduced into an hydroperoxide Fe^{III} complex, more easily than the initial Fe^{III} form of
22 the catalyst is reduced into its Fe^{II} form. Product selection – H₂O₂ vs. H₂O – occurs at this stage, being more
23 favorable to H₂O₂ in the heterogeneous case than in the homogeneous case. The hydroperoxide Fe^{III} complex is
24 then reduced into its Fe^{II} form at a more negative potential, giving rise to the second catalytic wave. Product
25 selection occurs at this stage, being more favorable to H₂O₂ in the heterogeneous case than in the homogeneous
26 case.
27
28
29
30
31
32
33
34
35
36
37

38 Estimation of the intrinsic reactivity during the early stages of the reaction sequence – formation of the initial
39 Fe^{II}-O₂ adduct and protonation – reveals that the reaction is more than one order of magnitude faster at the
40 adsorbed state than in solution. A likely interpretation of this observation relates to a better ligation by ligands
41 present on the GC surface than by the ligands available in solution. This also falls in lines with other
42 experimental data concerning half-wave potentials and product selectivity.
43
44
45
46
47
48
49

50 **Supporting Information**

51 Experimental details, establishment of the Pourbaix diagram relationship, analysis of the RDE voltammetry of
52 catalytic systems, estimation of H₂O₂ reduction rate constant, proof of equations (1-5). This material is available
53 free of charge via the Internet at <http://pubs.acs.org>.
54
55
56
57
58
59
60

References and Notes

1. He, Q.; Mugadza, T.; Kang, X.; Zhu, X.; Chen, S.; Kerr, J.; Nyokong, T. *J. Power Sources* **2012**, *216*, 67.
2. Savéant, J.-M. *Chem. Rev.* **2008**, *108*, 2348.
3. Jaouen, F.; Proietti, E.; Lefevre, M.; Chenitz, R.; Dodelet, J.-P.; Wu, G.; Chung, H. T.; Johnston, C. M.; Zelenay, P. *Energy Environ. Sci.* **2011**, *4*, 114.
4. Boulatov, R (2009) Metalloporphyrin catalysts for oxygen reduction. In Fuel cell catalysis: a surface science approach; Koper, M. T., Ed.; John Wiley & Sons: Hoboken, NJ, 2009 pp. 637-693.
5. (a) Carver, C. T.; Matson, B. D.; Mayer, J. M. *J. Am. Chem. Soc.* **2012**, *134*, 5444. (b) Matson, B. D.; Carver, C. T.; Von Ruden, A.; Yang, J. Y.; Raugei, S.; Mayer, J. M. *Chem. Comm.* **2012**, *48*, 11100. (c) Rigsby, M. L.; Wasylenko, D. J.; Pegis, M. L.; Mayer, J. M. *J. Am. Chem. Soc.* **2015**, *137*, 4296.
6. (a) Samanta, S.; Sengupta, K.; Mitra, K.; Bandyopadhyay, S.; Dey, A. *Chem. Comm.* **2012**, *48*, 7631. (b) Samanta, S.; Mitra, K.; Sengupta, K.; Chatterjee, S.; Dey, A. *Inorg. Chem.* **2013**, *52*, 1443. (c) Sengupta, K.; Chatterjee, S.; Samanta, S.; Bandyopadhyay, S.; Dey, A. *Inorg. Chem.* **2013**, *52*, 2000. (d) Samanta, S.; Mitra, K.; Sengupta, K.; Chatterjee, S.; Dey, A. *Inorg. Chem.* **2013**, *52*, 1443. (e) Sengupta, K.; Chatterjee, S.; Samanta, S.; Dey, A. *Proc. Natl. Acad. Sci. USA* **2013**, *110*, 8431. (f) Chatterjee, S.; Sengupta, K.; Samanta, S.; Das, P. K.; Dey, A. *Inorg. Chem.* **2015**, *54*, 2383.
7. Forshey, P. A. ; Kuwana, T. *Inorg. Chem.* **1981**, *20*, 693.
8. Shi, C. ; Anson, F. C. *Inorg. Chem.* **1990**, *29*, 4298.
9. *Handbook of Chemistry and Physics*, 82st ed.; CRC Press: Boca Raton, FL, 2001-2002, p. 8-87.
10. (a) Forshey, P. A. ; Kuwana, T. *Inorg. Chem.* **1983**, *22*, 699-707. (b) Pasternack, R. F. ; Lee, H. ; Malek, P. ; Spencer, C. J. *Inorg. Nucl. Chem.* **1977**, *39*, 1865-1870. (c) Gandini, S. C. M. ; Vidoto, E. A. ; Nascimento,

O. R. ; Tabak, M. J. *Inorg. Biochem.* **2003**, *94*, 127-137. (d) Rywkin, S. ; Hosten, C. M. ; Lombardi, J. R. ; Birke, R. L. *Langmuir*, **2002**, *18*, 5869-5880.

11. Wopschall, R. H.; Shain, I. *Anal. Chem.* **1967**, *39*, 1514.

12. (a) Albery, W. J.; Hitchman, M. L. *Ring-Disc Electrodes* Ed. Clarendon Press, Oxford, 1971, Chap 6. (b) calibration of the RRDE electrode with a test compound (potassium ferricyanure) leads to $N_{eff} = 0.4$ vs. 0.37 from the manufacturer.

13. An analysis of the RDE voltammetry of catalytic systems is provided in the Supporting Information section.

14. Albery, W. J.; Bruckenstein, S. *Trans. Faraday Soc.* **1966**, *62*, 1946-1954.

15. *Handbook of Chemistry and Physics*, 82st ed.; CRC Press: Boca Raton, FL, 2001-2002, p. 6-3.

16. (a) When homogeneous catalysis reaches the pure kinetic regime ^{16b} as the result of mutual compensation of the catalytic reaction and of the catalyst diffusion, the current potential response is the same in cyclic voltammetry and in RDEV. The characteristics of the current-potential curve that have been established in the first case ^{16b,c} are therefore applicable in the second. (b) Savéant, J.-M. *Elements of molecular and biomolecular electrochemistry: an electrochemical approach to electron transfer chemistry*; John Wiley & Sons: Hoboken, NJ, 2006. pp. 109. (c) Costentin, C ; Savéant, J.-M. *ChemElectroChem* **2014**, *1*, 1226.

17. *pH* s higher than 3.8 were excluded for reasons discussed in section 1.

18. Savéant, J.-M. *Elements of molecular and biomolecular electrochemistry: an electrochemical approach to electron transfer chemistry*; John Wiley & Sons: Hoboken, NJ, 2006. pp. 96-102.

19. (a) In the heterogeneous catalysis the diffusion current for H₂O₂ removal from the disk electrode is expressed as: ^{19b} $i_d^{H_2O_2} = 2 \times 0.201 F \pi r_1^2 D_{H_2O_2}^{2/3} \nu^{-1/6} \sqrt{\omega} [H_2O_2]_{x=0}$ where r_1 is the radius of the disk, ν the

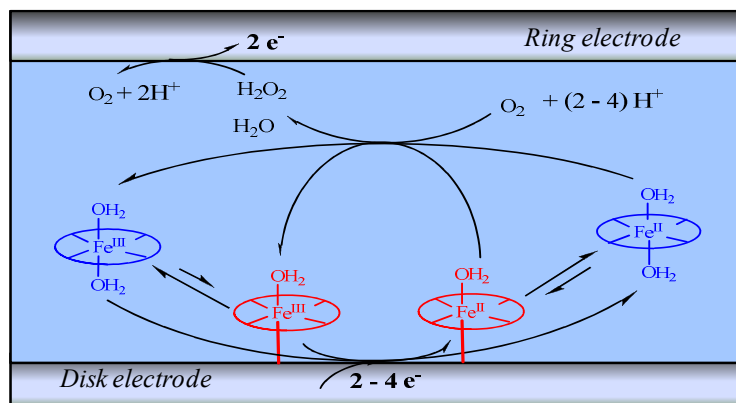
1
2 viscosity of water, ω the rotation rate in rpm, $[\text{H}_2\text{O}_2]_{x=0}$ the H_2O_2 concentration at the electrode surface.
3
4
5 Taking into account the collection efficiency N_{eff} and that the maximal ring current (with $r_1 = 5.6$ mm) due to
6
7 heterogeneous catalysis at 2500 rpm is ca. 50 μA , we obtain that the maximal concentration of H_2O_2 generated
8
9 by the heterogeneous catalysis in the reaction layer during the homogeneous catalysis is ca. 0.2 mM. Because
10
11 $k_3 = 10^4 \text{ M}^{-1}\text{s}^{-1}$ we end up with $k_1^{\text{hom}} \gg k_3[\text{H}_2\text{O}_2]$ in agreement with the experimental observation of the
12
13 homogeneous disk current to be proportional to $\sqrt{[\text{O}_2]}$ and the high selectivity of the homogeneous catalysis
14
15 toward H_2O production. (b) Jia, Z.; Yin, G.; Zhang, J. *Rotating Ring-Disk Electrode Method in Rotating*
16
17 *Electrode Methods and Oxygen Reduction Electrocatalysts*. Ed. Elsevier B. V. 2014, Chap 6.
18
19
20
21
22
23

24 20. (a) the fact that only a minor part of the catalyst molecules present actually partake to catalysis in the
25
26 homogeneous case may be consider as a serious drawback as compared to the heterogeneous case where all the
27
28 molecules present on the surface are involved (at least with thin films). It may however been viewed as an
29
30 advantage if the catalyst is not very stable, since the molecules outside the reaction-diffusion layer can then act
31
32 as backup for the replacement of degraded catalyst molecules.^{20b} (b) Costentin, C.; Passard, G.; Savéant, J.-M.
33
34 *J. Am. Chem. Soc.* **2015**, *137*, 5461.
35
36
37
38

39 21. (a) such as carboxylate and hydroxyl groups.^{21b} (b) McCreery, R. L. *Chem. Rev.*, **2008**, *108*, 2646.
40
41

42 22. Lexa, D.; Momenteau, M.; Savéant, J.-M.; Xu, F. *Inorg. Chem.* **1986**, *25*, 4857 and references cited
43
44 therein.
45
46
47

48 23. Renault, C.; Nicole, L.; Sanchez, C.; Costentin, C.; Balland, V.; Limoges, B. *Phys. Chem. Chem. Phys.*
49
50 **2015**, *17*, 10592.
51
52
53
54
55
56
57
58
59
60



TOC